acknowledge the Institute of Instrumental Analysis of Kitasato University, School of Pharmacy for its facilities.

References and notes

1. Dhawan, B. N.; Cesselin, F.; Raghubir, T.; Reisine, T.; Bradley, P. B.; Portoghese, P. S.; Hamon, M. *Pharmacol. Rev.* **1996**, *48*, 567 (and references cited therein).
2. Fujii, H.; Nagase, H. *Curr. Med. Chem.* **2006**, *13*, 1109 (and references cited therein).
3. (a) Rios, C. D.; Jordan, B. A.; Gomes, I.; Devi, L. A. *Pharmacol. Ther.* **2001**, *92*, 71; (b) Angers, S.; Salahpour, A.; Bouvier, M. *Annu. Rev. Pharmacol. Toxicol.* **2002**, *42*, 409; (c) Prinster, S. C.; Hague, C.; Hall, R. A. *Pharmacol. Rev.* **2005**, *57*, 289.
4. Levac, B. A. R.; O'Dowd, B. F.; George, S. R. *Curr. Opin. Pharmacol.* **2002**, *2*, 76.
5. Kieffer et al. reported that there was no evidence for the presence of the G-protein-coupled ε receptor as a monomer based on the results of [^{35}S]GTPγS binding assay using the preparations obtained from triple opioid receptor knockout mice. They described that the ε receptor may result from opioid receptor dimerization or from heterodimerization of an opioid receptor with another partner. Contet, C.; Matifas, A.; Kieffer, B. L. *Eur. J. Pharmacol.* **2004**, *492*, 131.
6. Fujii, H.; Narita, M.; Mizoguchi, H.; Murachi, M.; Tanaka, T.; Kawai, K.; Tseng, L. F.; Nagase, H. *Bioorg. Med. Chem.* **2004**, *12*, 4133.
7. Fujii, H.; Narita, M.; Mizoguchi, H.; Hirokawa, J.; Kawai, K.; Tanaka, T.; Tseng, L. F.; Nagase, H. *Bioorg. Med. Chem. Lett.* **2004**, *14*, 4241.
8. Watanabe, A.; Kai, T.; Nagase, H. *Org. Lett.* **2006**, *8*, 523.
9. Contreras, J.-M.; Bourguignon, J.-J. The Practice of Medicinal Chemistry. In Wermth, C. G., Ed., 2nd ed.; Academic Press: London, 2003; pp 251–273.
10. Portoghese, P. S.; Nagase, H.; Lipkowski, A. W.; Larson, D. L.; Takemori, A. E. *J. Med. Chem.* **1988**, *31*, 836.
11. Stoddart, J. F.. In *Comprehensive Organic Chemistry*; Springer: Berlin, 1979; Vol. 1. pp 1002–1003.
12. Crystallographic data of compound **8** have been deposited with the Cambridge Crystallographic Data Center as supplementary Publication No. CCDC 705154. These data can be obtained free of charge from the Cambridge Crystallographic Data Center via www.ccdc.cam.ac.uk/data_request/cif.
13. Nagase, H.; Watanabe, A.; Nemoto, T.; Yamamoto, N.; Osa, Y.; Sato, N.; Yoza, K.; Kai, T. *Tetrahedron Lett.* **2007**, *48*, 2547.
14. β-Endorphin was reported to show agonism for μ and putative ε opioid receptor in [^{35}S]GTPγS binding assay. Mizoguch, H.; Narita, M.; Nagase, H.; Tseng, L. F. *Life Sci.* **2000**, *67*, 2733.
15. Portoghese, P. S. *Trends Pharmacol. Sci.* **1989**, *10*, 230.
16. (a) Portoghese, P. S.; Sultana, M.; Nagase, H.; Takemori, A. E. *J. Med. Chem.* **1998**, *31*, 281; (b) Nagase, H.; Kawai, K.; Hayakawa, J.; Wakita, H.; Mizusuna, A.; Matsuura, H.; Tajima, C.; Takezawa, Y.; Endo, T. *Chem. Pharm. Bull.* **1998**, *46*, 1695; (c) Kawai, K.; Hayakawa, J.; Miyamoto, T.; Imamura, Y.; Yamane, S.; Wakita, H.; Fujii, H.; Kawamura, K.; Matsuura, H.; Izumimoto, N.; Kobayashi, R.; Endo, T.; Nagase, H. *Bioorg. Med. Chem.* **2008**, *16*, 9188.
17. Nogrady, T. In *Medicinal Chemistry, A Biochemical Approach*; Nogrady, T., Ed.; Springer: Berlin, 1985. pp 68–69.

J Pharmacol Sci 111, 60 – 72 (2009)

Journal of Pharmacological Sciences

Full Paper

Morphine, Oxycodone, and Fentanyl Exhibit Different Analgesic Profiles in Mouse Pain Models†

Kazuhisa Minami[1], Minoru Hasegawa[1], Hisanori Ito[1], Atsushi Nakamura[1], Takako Tomii[1], Mitsunobu Matsumoto[2], Satoshi Orita[2], Syuichi Matsushima[3], Takako Miyoshi[3], Koichi Masuno[3], Mikinori Torii[3], Katsumi Koike[1], Shinji Shimada[1], Toshiyuki Kanemasa[1], Tsuyoshi Kihara[1], Minoru Narita[4], Tsutomu Suzuki[4], and Akira Kato[1,*]

[1]*Pain & Neurology, Discovery Research Laboratories, Shionogi & Co., Ltd., 1405 Gotanda, Koka-cho, Koka, Shiga 520-3423, Japan*
[2]*Allergy & Cancer, Discovery Research Laboratories, Shionogi & Co., Ltd., 5-12-4, Sagisu, Fukushima-ku, Osaka 553-0002, Japan*
[3]*Drug Safety Evaluation, Developmental Research Laboratories, Shionogi & Co., Ltd., 3-1-1 Futaba-cho, Toyonaka, Osaka 561-0825, Japan*
[4]*Department of Toxicology, Hoshi University School of Pharmacy and Pharmaceutical Sciences, 2-4-41 Ebara, Shinagawa-ku, Tokyo 142-8501, Japan*

Received May 4, 2009; Accepted July 15, 2009

Abstract. Morphine, oxycodone, and fentanyl are clinically prescribed drugs for the management of severe pain. We investigated whether these opioids possess different efficacy profiles on several types of pain in mouse pain models. When the three opioids were tested in the femur bone cancer model, all of them significantly reversed guarding behavior, whereas the effects on limb-use abnormality and allodynia-like behavior differed among the opioids. Particularly, although oxycodone (5 – 20 mg/kg) and fentanyl (0.2 mg/kg) significantly reversed limb-use abnormality, not even a high dose of morphine (50 mg/kg) could reverse it. When the effects of these opioids were examined in a sciatic nerve ligation (SNL) model of neuropathic pain, oxycodone was the most effective, producing an antinociceptive effect without affecting the withdrawal threshold of sham-treated animals. When the effects of these opioids were examined with the tail-flick test using naive animals, oxycodone, morphine, and fentanyl exhibited antinociceptive effects on thermal nociception. These results show that the three opioids exhibit different efficacy outcomes in multiple pain models and that the efficacy profile of oxycodone does not overlap those of morphine and fentanyl.

Keywords: oxycodone, morphine, fentanyl, neuropathic pain-like state, bone cancer pain

Introduction

Morphine, oxycodone, and fentanyl are clinically prescribed opioids for the management of severe pain. These opioids possess strong antinociceptive effects on various types of pain related to abnormal physical conditions (1); however, certain types of pain are difficult to control with an opioid. For example, neuropathic pain, caused by nerve injury, does not respond effectively to opioids (2). As a result, tricyclic antidepressants (3) and/or serotonin/noradrenaline re-uptake inhibitors (4) are prescribed for this type of pain. Bone cancer pain is another example in which treatment with opioid alone is often insufficient (5 – 7). Although the doses of opioid may be gradually increased to obtain better pain relief, adverse effects such as drowsiness or respiratory depression become problematic, as those adverse effects significantly affect the patient's quality of life (8 – 10). To more effectively manage cancer pain, a combination of an opioid and a non-opioid analgesic

†Part of the present study has been published previously in "Oncology. 2008;74 Suppl 1:55 – 60" as a proceeding for The Fourth Asia Pacific Symposium on Pain Control.

*Corresponding author. akira_kato@shionogi.co.jp

Published online in J-STAGE on September 4, 2009 (in advance)
doi: 10.1254/jphs.09139FP

such as an anticonvulsant, an antidepressant, or a local anesthetic has been preferred for a better clinical outcome (11, 12).

Among several opioids, oxycodone has recently been recommended for the treatment of cancer and non-cancer pain (13). Several clinical reports have shown that oxycodone effectively relieved pain in patients suffering from bone cancer pain or neuropathic pain induced by post-herpetic neuralgia (PHN) or diabetic neuropathy (DNP). For example, Bercovitch and Adunsky (14) reported that a high dose of oxycodone (e.g., 231 mg/day) could relieve bone cancer pain, and Watson et al. reported that controlled-release oxycodone was effective to manage pain induced by PHN (15) and DNP (16).

The antinociceptive effects of oxycodone, morphine, and fentanyl have been studied in several animal pain models. These opioids exhibited the significant antinociceptive effects, as measured by the tail-flick test, on pain caused by thermal stimuli (17). In the mouse sciatic nerve ligation (SNL) model, oxycodone has been shown to reverse the nociceptive pain caused by mechanical stimuli (18). Furthermore, in a mouse femur bone cancer (FBC) model, which showed similar pathological symptoms to human bone metastasis, morphine and fentanyl were reported to exhibit antinociceptive effects on several pain-related behaviors (19). Although those studies showed that these opioids were effective on several different types of pain, only a few studies have directly compared the pharmacological efficacy of the three opioids in animal pain models (17). For an appropriate opioid use, it is important to understand the pharmacological profile of each opioid in various types of pain.

In the present study, the pharmacological efficacies of morphine, oxycodone, and fentanyl were investigated in the FBC and the SNL models as well as in the tail-flick test. Our results showed that morphine, oxycodone, and fentanyl exhibited different efficacy profiles in some of the mouse pain models. Among the three opioids, oxycodone showed the most favorable analgesic effect in both the FBC and the SNL models.

Materials and Methods

Experimental animals

The experiments were performed using male C3H/HeN mice (CLEA Japan, Inc., Tokyo) and male ICR mice (Japan SLC, Inc., Shizuoka), weighing 18 – 23 and 20 – 25 g, respectively. The mice were housed in a vivarium with a 12-h alternating light-dark cycle and were given food and water ad libitum. All procedures were approved by the Animal Care and Use Committee of Shionogi Research Laboratories, Osaka, Japan.

Drug administration

Morphine hydrochloride (produced by Shionogi & Co., Ltd., Osaka), oxycodone hydrochloride (produced by Shionogi & Co., Ltd.), fentanyl citrate (Fentanyl injection; Daiichi-Sankyo Co., Ltd., Tokyo) were each dissolved in saline solution. The drug solutions were freshly prepared on each experimental day. Oxycodone, morphine, or fentanyl was administered subcutaneously 30 min before pain assessment.

The FBC model

For the FBC model, NCTC 2472 tumor cells (American Type Culture Collection, Manassas, VA, USA) were injected into the medullary cavity of the distal femur of C3H/HeN mice (20). The NCTC 2472 cells were maintained in Dulbecco's Modified Eagle's Medium (Invitrogen, Inc., Carlsbad, CA, USA), supplemented with 10% fetal bovine serum (Invitrogen, Inc.), 100 units/mL penicillin, and 100 μg/mL streptomycin (Invitrogen, Inc.); and they were cultured at 37 ± 0.2°C in a humidified atmosphere of 5% CO_2. The NCTC 2472 tumor cells were transfected with the luciferase gene in pUSEamp (Upstate, Lake Placid, NY, USA), using Lipofectamine 2000 (Invitrogen, Inc.). Transfected cells were selected by growth in medium containing 1 mg/mL G418 (Invitrogen, Inc.). Luciferase-expressing colonies were confirmed by measuring luciferase activity using an IVIS imaging system 200 (Xenogen Corp., Alameda, CA, USA) and were isolated by using cloning rings.

Tumor cells were injected following the protocol described previously by Honore et al. (20) with slight modification. In brief, mice were anesthetized with 0.2% xylazine (Selactar; Bayer Medical, Ltd., Tokyo) and 1% ketamine (Ketalar; Daiichi Sankyo Co., Ltd.), and a left knee arthrotomy was performed. Wild-type or luciferase-transfected tumor cells [1×10^5 cells in 5 μl of Hank's balanced salt solution (Invitrogen, Inc.)] were injected directly into the medullary cavity of the distal femur, and the drilled hole in the bone was closed with resin cement (ADFA; Shofu Inc., Kyoto). In the sham group, 5 μL of Hank's balanced salt solution was injected directly into the medullary cavity of the distal femur, and the drilled hole was repaired in the same manner.

Evaluations of tumor growth and bone destruction in the FBC model

Tumor-implanted mice were visualized by whole-body luciferase imaging with the IVIS imaging system 200 (Xenogen Corp.). Briefly, one milligram of potassium salt of D-luciferin dissolved in 0.1 ml phosphate-buffered saline (PBS, Invitrogen, Inc.) was injected intrave-

nously to mice using 27-gauge syringes. Then the mice were kept under anesthesia with isoflurane. Immediately starting after the luciferin injection, images were collected for 60 s. Relative tumor metastasis burden in mice was calculated with the Living Image software version 2.50 (Xenogen Corp.).

On 3, 7, 10, and 14 days after tumor implantation, the mice were anesthetized with diethylether and refluxed with 10% neutral buffered formalin. The femur bone was removed and fixed with 10% neutral buffered formalin for 2 days. The 3-μm–thick cross-sections of femur bone were stained by hematoxylin and eosin for histological analyses.

The extent of tumor-induced bone destruction (osteolysis) was monitored by X-ray radiography on 7, 14, and 21 days after tumor implantation. The mice were anesthetized with diethylether and refluxed with 10% neutral buffered formalin. Then the femur bone was removed and fixed with 10% neutral buffered formalin for 2 days. Removed femur bone was placed on wrapped films (Fuji Industrial X-ray Film FR; Fuji Photo Film, Kanagawa) and exposed to X-irradiation at 35 kV for 70 s using a Soft X-ray SOFRON Apparatus (Sofron, Tokyo).

Behavioral analysis in the FBC model

The behavioral analysis was preformed following the protocol described previously by Lugar et al. (21). The pain-related behaviors in the FBC model were evaluated before and after drug administration on 14 days after tumor implantation. The experimental and sham animals were evaluated for ongoing pain based on guarding behavior, for ambulatory pain based on limb-use abnormality, and for allodynia-like behavior based on the von Frey monofilament test. Guarding behavior and limb-use abnormality were assessed in the same animals, and allodynia-like pain was assessed in a separate set of animals.

The mice were placed in a clear plastic observation box and allowed to habituate for 15 min. Then the spontaneous guarding behavior was assessed during a 2-min observation period. The lifting time of the hind paw on the ipsilateral side during ambulation was measured as guarding behavior. Limb-use abnormality on the ipsilateral side during spontaneous ambulation was scored on a scale of 0 to 4: 0, normal use of limb; 1, slight limp; 2, clear limp; 3, partial non-use of limb; and 4, complete non-use of limb. Allodynia-like behavior was measured by the withdrawal threshold upon application of von Frey monofilament stimulation to the plantar surface of the hind paw (pressures: 0.008, 0.02, 0.04, 0.07, 0.16, 0.4, 0.6, and 1 g). The up-down method of von Frey monofilament test (22) was used in the present study. Briefly, the von Frey filaments were applied to the ipsilateral side of the hind paw for the maximum period of 4 s, and withdrawal response was observed. The 0.07-g stimulus was applied first. When withdrawal response to a given filament was observed, a one step thinner filament (a weaker stimulation) was applied. The same procedure was continued until the descending monofilament stimulation no longer induced the behavioral response. When no response was observed by the monofilament stimulation, a one step thicker monofilament (a stronger stimulation) was applied again to confirm the positive response. After that, no response was again confirmed by the one step thinner monofilament to complete the test, and the weakest stimulation that caused the positive response was taken as the threshold value. The mice showing the threshold change from 0.07 or 0.16 g (before tumor implantation) to 0.008 g (on the 14 days after tumor implantation) were used in the experiments.

Experiments using the SNL model

For the SNL model, ICR mice were anesthetized with 3% isoflurane, and a ligature was tied tightly with 8-0 silk suture around approximately 1/3 to 1/2 the diameter of the sciatic nerve on the left hind paw side (ipsilateral side), as described previously (23). In sham-operated mice, the nerve was exposed, but the nerve ligation was not performed. At 7 days after surgery, the drug efficacies were evaluated in these animals. The neuropathic pain-like state was assessed by measuring the withdrawal threshold using von Frey monofilament stimulation applied to the plantar surface of the hind paw (pressures: 0.008, 0.02, 0.04, 0.07, 0.16, 0.4, 0.6, and 1 g). The up-down method of the von Frey monofilament test was used as described above. The mice showing the threshold change from 0.07 or 0.16 g (before the surgery) to below 0.02 g (on the 7 days after the nerve ligation) were used in the experiments.

Assessment of anti-thermal nociception

The assessment of anti-thermal nociception was performed by the tail-flick test (Ugo Basile, Comerio, VA, Italy). The intensity of the heat stimulus was adjusted so that the intact animal flicked its tail within 2 – 4 s after stimulus application. The tail-flick response was measured before and after drug administration, and the cut-off time was set at 10 s to avoid injury to the tail.

Statistical analyses

All data are reported as values of the mean ± S.E.M. SAS software ver. 8 was used to perform the statistical analysis. One-way ANOVA was used to compare continuous data, including tail-flick latency and guarding

behavior, among the experimental groups. A Kruskall-Wallis test was used to compare discontinuous data, including neuropathic pain-like state, limb-use abnormality, and allodynia-like behavior, among the experimental groups. For multiple comparisons, Dunnett's test (for tail-flick latency and guarding behavior) or Steel's test (for neuropathic pain-like state, limb-use abnormality, and allodynia-like behavior) was used. For comparisons between two groups, Student's *t*-test (for guarding behavior) or the Wilcoxon signed-rank test (for limb-use abnormality and allodynia-like behavior) was used. A probability value (P) of <0.05 was considered to be statistically significant. The dose producing 50% of the effect (ED_{50}) was determined by inverse prediction based on the regression analysis.

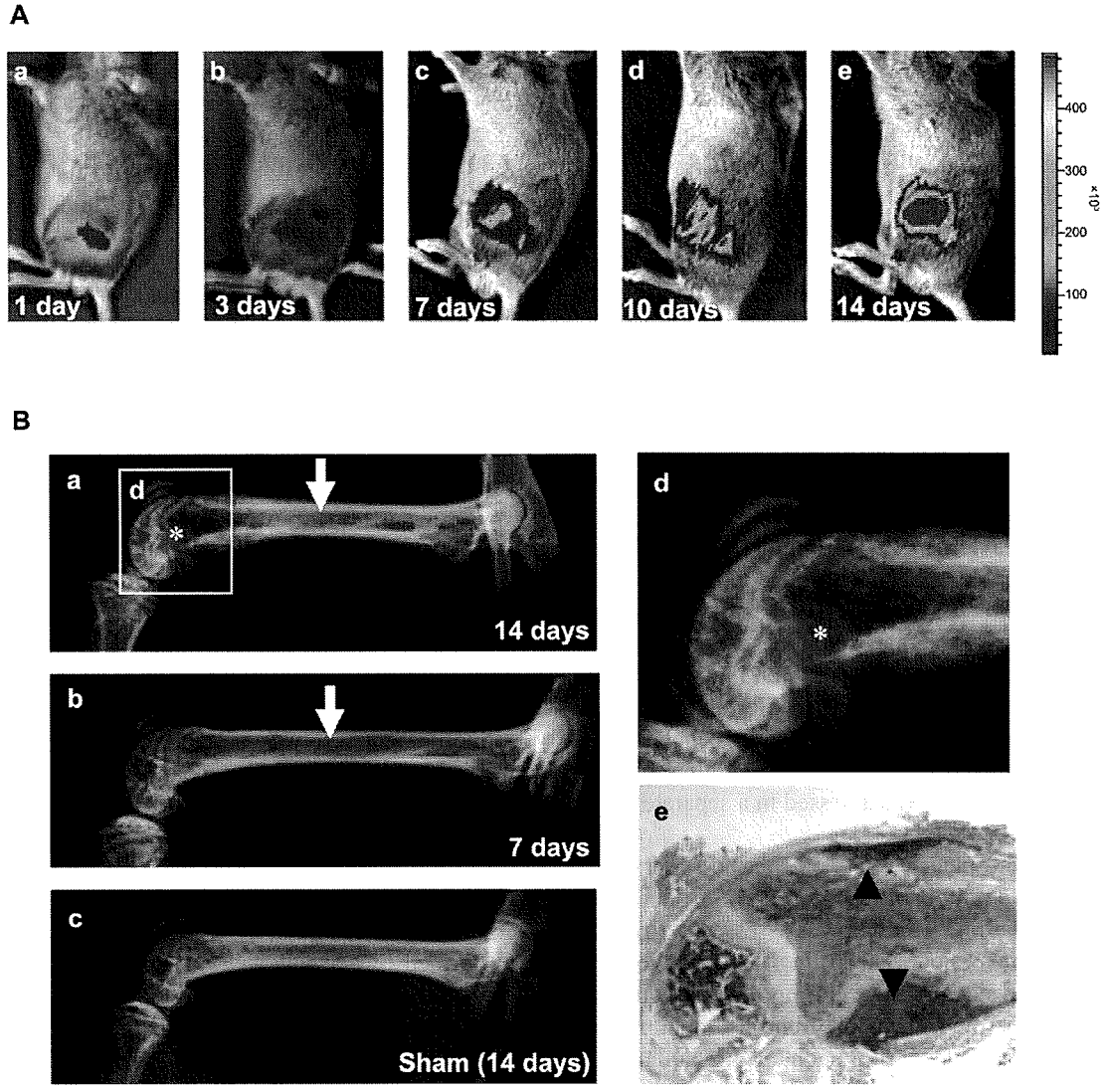

Fig. 1. Histological analysis of tumor growth. A: Luciferase gene-transfected NCTC2472 cells were implanted into the intramedulla of left femur bone (10^5 cells/5 μl). Luminescence was measured by IVIS®200 within 5 min after i.v. injection of luciferin (1 mg/ml) at 0.2 ml/mouse at 1 (a), 3 (b), 7 (c), 10 (d), and 14 (e) days after tumor implantation. The color, which indicates the intensity of photon emission, changes from blue to red as tumor cells grow. B: Radiographs show the left femur bone of the FBC model at 14 (a) and 7 (b) days in the tumor implanted-group and at 14 days in the sham-treated group (c), and the radiograph (d) expanded to show the distal part of the femur bone, which corresponds to the area surrounded by the square in photo Ba. The arrows and asterisk in the radiographs indicate the area of tumor implantation and bone destruction, respectively. The photomicrograph (e) shows the distal part of the femur bone, which is stained by hematoxilin and eosin. The arrow heads in the photomicrograph indicate the tumor cells that invade between the periosteum and the cortical bone.

Results

The histological analysis of tumor growth in the FBC model

The growth of the implanted tumor cells was investigated in the FBC model by monitoring the photon emission from the tumor cells stably expressing luciferase (Fig. 1A). On the first day after the tumor implantation, the photon emission was restricted within the implanted area with the low emission level (Fig. 1Aa). The progressive tumor growth was observed for 14 or more days after tumor implantation. The photon emission was not observed throughout the body even on 14 days after tumor implantation, suggesting that the tumor cells were retained within a relatively restricted area around the femur (Fig. 1A). Histological and X-ray analyses were applied to observe the anatomical changes in the femur bone, and we confirmed that the tumor cells progressively grew in the intramedulla and started invading the trabecular bone around 7 days after tumor implantation (Table 1). On 10 days after tumor implantation, the trabecular bone was filled with tumor cells (Table 1 and Fig. 1Be), which reached to the zone of ossification of the femur, followed by further invasion into the part between the periosteum and cortical bone on at 14 days after tumor implantation (see the black arrow heads in Fig. 1Be). The X-ray radiographs indicated that bone destruction occurred in the distal part of the femur bone by 14 days after tumor implantation (see the asterisks in Fig. 1: Ba and Bd). The radiographs and photomicrograph observations confirmed that there was invasion of the tumor cells at the area where bone destruction was observed. No significant change in the bone histology was observed in the sham-treated group on 14 days after the surgery (Fig. 1Bc).

Table 1. Histological analysis of tumor growth in the femur bone

	Tumor cells in femur bone	
	Extent	Observed area
3 days	±	Intramedulla
7 days	±, +, ++, +++	Intramedulla
10 days	+++	Intramedulla and trabecular bone
14 days	+++	Intramedulla Trabecular bone Between priosteum and cortical bone

The symbols in the table indicate the extent of tumor cell invasion as follows: (±) less than 10%, (+) 10% – 30%, (++) 30% – 60%, and (+++) over 60%.

The correlation between the tumor growth and pain-related behaviors in the FBC model

To evaluate the tumor growth level in the FBC model, the photon intensity was measured from the images captured by the IVIS. The levels of the emitted photon

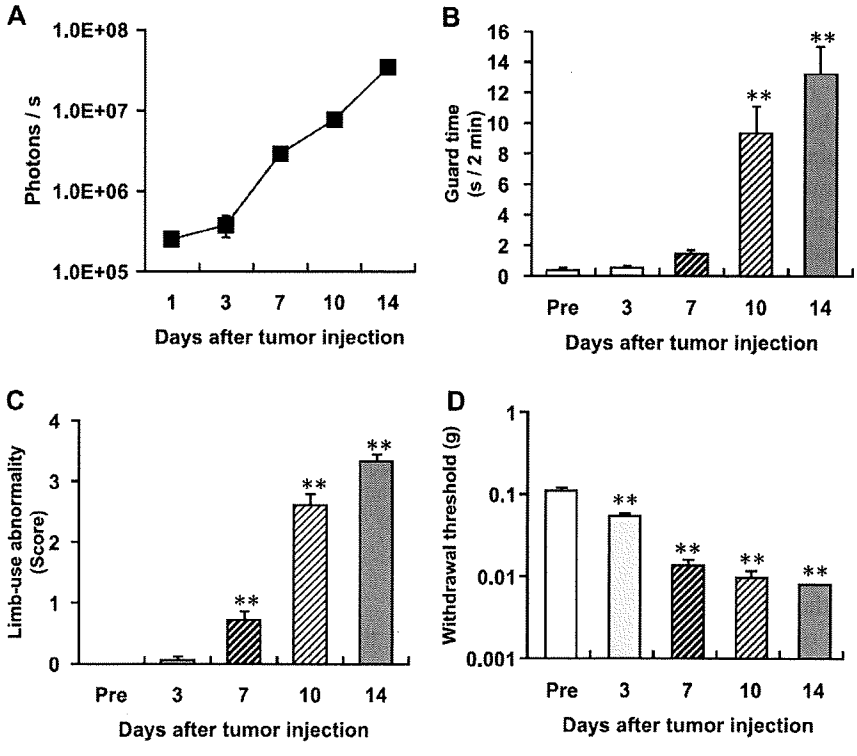

Fig. 2. The correlation between the tumor growth and the observed pain-related behaviors. The photons of luminescence captured in the IVIS imaging system were calculated by the Living Image Software on days 1, 3, 7, 10, and 14 after tumor implantation. The data represents the mean ± S.E.M. (n = 18) (A). Guarding (B), limb-use abnormality (C), and allodynia-like behavior (D) were measured at pre-implantation and on days 3, 7, 10, and 14 after tumor implantation. Each column and vertical bar show the mean ± S.E.M. of 18 measurements. $^{**}P<0.01$, compared with the pre-implantation (Pre) group (Dunnett's test). Modified from Ref. 37 (proceeding for The Fourth Asia Pacific Symposium on Pain Control, Kuala Lumpur, November 2 – 4, 2007) with permission from S. Karger AG, Basel.

intensity gradually increased after the tumor cell implantation, and the level at 3 days after tumor implantation was approximately 1.5-fold of the level on day 1, 11-fold at day 7, 31-fold at day 10, and 135-fold at 14 days after tumor implantation (Fig. 2A). The previous studies showed that several pain-related behaviors were observed in the FBC model. Guarding behavior is thought to indicate ongoing pain, limb-use abnormality is thought to represent ambulatory pain, and an allodynia-like behavior is thought to represent touch-evoked pain in this model (21). We, therefore, investigated whether these behaviors were correlated with tumor growth. The guard times were significantly prolonged at 10 and 14 days after tumor implantation compared with the values at pre-implantation (Fig. 2B). Similarly, animals also started to exhibit abnormal limb-use at 7 days after tumor implantation, and such abnormal behavior was more prominent in the later days (Fig. 2C). Allodynia was evaluated by measuring the paw withdrawal threshold in response to probing with von Frey monofilaments, and significant threshold drops were observed after the 3rd day post tumor implantation (Fig. 2D). These results showed that those pain-related behaviors were correlatively observed with tumor growth in this model.

Effects of oxycodone, morphine, and fentanyl in the FBC model

We tested the effects of oxycodone, morphine, and fentanyl in the FBC model. The effects of each opioid were assessed by observing three pain-related behaviors: guarding behavior, limb-use abnormality, and allodynia-like behavior. Figure 3 shows that all three opioids similarly reduced the guarding time in the FBC model group without affecting the sham-treated group. In contrast, the antinociceptive effects on ambulatory pain differed among the opioids (Fig. 4). Within the range of doses that did not affect the sham-treated group, only oxycodone at 5 mg/kg exhibited a significant analgesic effect (Fig. 4). Although fentanyl at 0.2 mg/kg significantly improved the limb-use abnormality score, this dose of fentanyl also affected the sham-treated group. Morphine did not improve the limb-use abnormality score, even at the highest dose tested (50 mg/kg, s.c.) (Fig. 4). The effects of the opioids on allodynia-like behavior were measured using the von Frey monofilament test. Oxycodone (5 – 20 mg/kg, s.c.), morphine (50 mg/kg, s.c.), and fentanyl (0.075 – 0.2 mg/kg, s.c.) significantly reversed the decrease of the paw withdrawal threshold, indicating that all three opioids effectively reversed allodynia-like behavior (Fig. 5). However, the effective doses of morphine (50 mg/kg, s.c.) and fentanyl (0.1 and 0.2 mg/kg, s.c.) were close to or at the

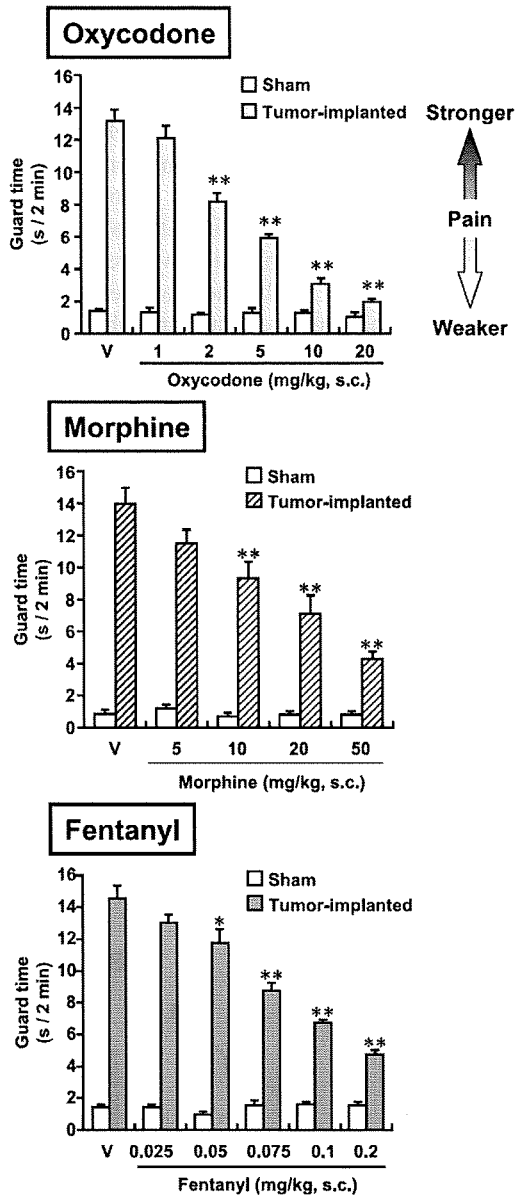

Fig. 3. The effects of oxycodone, morphine, and fentanyl on guarding behavior. The analgesic effects of oxycodone, morphine, and fentanyl on on-going pain in FBC model mice were evaluated based on guarding behavior. FBC model mice were used at 14 days after tumor implantation, and each opioid was administered subcutaneously 30 min before the measurement. Open and filled columns indicate the sham-treated and tumor-implanted groups, respectively. The columns and vertical bars show the means ± S.E.M. (n = 6 – 8). *$P<0.05$, **$P<0.01$, compared with vehicle (V) in the tumor-implanted group (one-way ANOVA and Dunnett's test).

doses that affected the paw withdrawal threshold in the sham-treated group, while oxycodone reversed the allodynia-like behavior without affecting the sham group (Fig. 5).

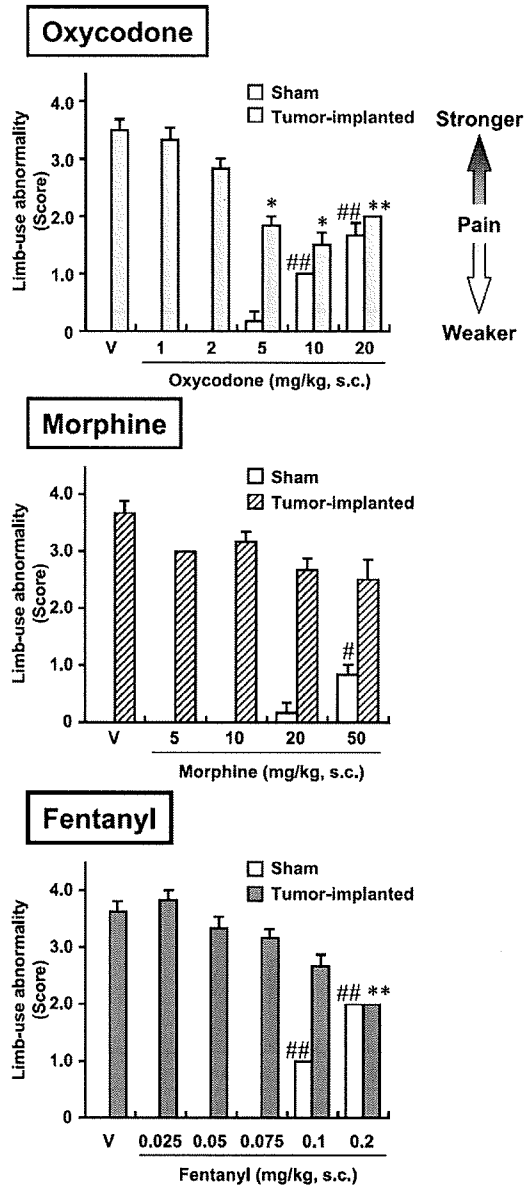

Fig. 4. The effects of oxycodone, morphine, and fentanyl on limb-use abnormality. The analgesic effects of oxycodone, morphine, and fentanyl on ambulatory pain in FBC model mice were evaluated based on limb-use abnormalities. FBC model mice were used at 14 days after tumor implantation, and each opioid was administered subcutaneously 30 min before measuring the limb-use abnormality score. Open and filled columns indicate the sham-treated and tumor-implanted groups, respectively. The columns and vertical bars show the means ± S.E.M (n = 6 – 8). *P<0.05, **P<0.01, compared with vehicle (V) in the tumor-implanted group (Kruskall-Wallis test and Steel's test). $^{\#}P$<0.05, $^{\#\#}P$<0.01, compared with vehicle (V) in the sham-treated group (Kruskall-Wallis test and Steel's test).

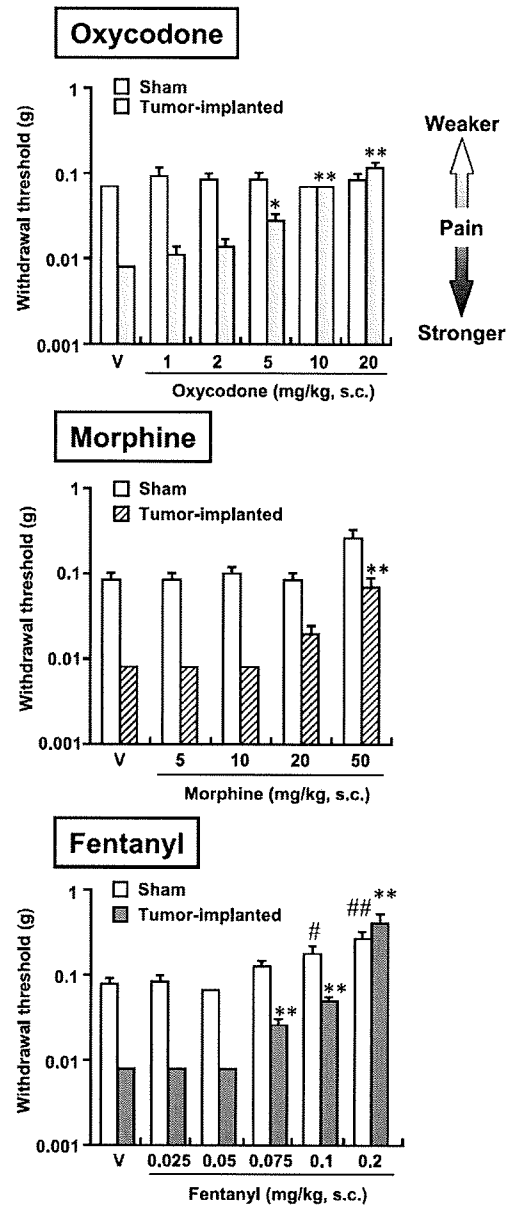

Fig. 5. The effects of oxycodone, morphine, and fentanyl on allodynia-like behavior. The effects of oxycodone, morphine, and fentanyl on allodynia-like behavior in FBC model mice were evaluated. FBC model mice were used 14 days after tumor implantation, and each opioid was administered subcutaneously 30 min before the measuring the withdrawal threshold in the von Frey monofilament test. Open and filled columns indicate sham-treated and tumor-implanted groups, respectively. The columns and vertical bars show the means ± S.E.M. (n = 6 – 8). *P<0.05, **P<0.01, compared with vehicle (V) in the tumor-implanted group (Kruskall-Wallis test and Steel's test). $^{\#}P$<0.05, $^{\#\#}P$<0.01, compared with vehicle (V) in the sham-treated group (Kruskall-Wallis test and Steel's test).

Effects of oxycodone, morphine, and fentanyl on a neuropathic pain-like state in SNL model mice

To evaluate the antinociceptive effects of oxycodone, morphine, and fentanyl on a neuropathic pain-like state, the withdrawal threshold to stimulation with von Frey monofilaments was measured in the hind paw of SNL

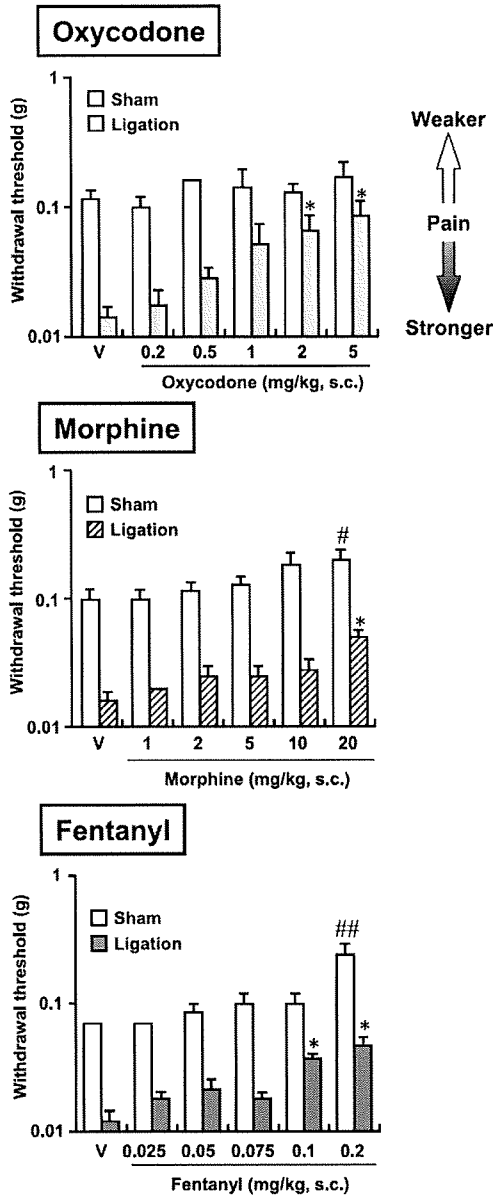

Fig. 6. The effects of oxycodone, morphine, and fentanyl on the neuropathic pain-like state. The antinociceptive effects of oxycodone, morphine, and fentanyl on a neuropathic pain-like state in sciatic nerve ligation (SNL) model mice were evaluated. Seven days after nerve ligation, each opioid was administered subcutaneously 30 min before measuring the withdrawal threshold to stimulation with von Frey monofilaments. Open and filled columns indicate the sham-treated and SNL groups, respectively. The columns and vertical bars show the means ± S.E.M. (n = 8). $^{*}P<0.05$, compared with vehicle (V) in the SNL group (Kruskall-Wallis test and Steel's test). $^{\#}P<0.05$, $^{\#\#}P<0.01$, compared with vehicle (V) in the sham-operated group (Kruskall-Wallis test and Steel's test).

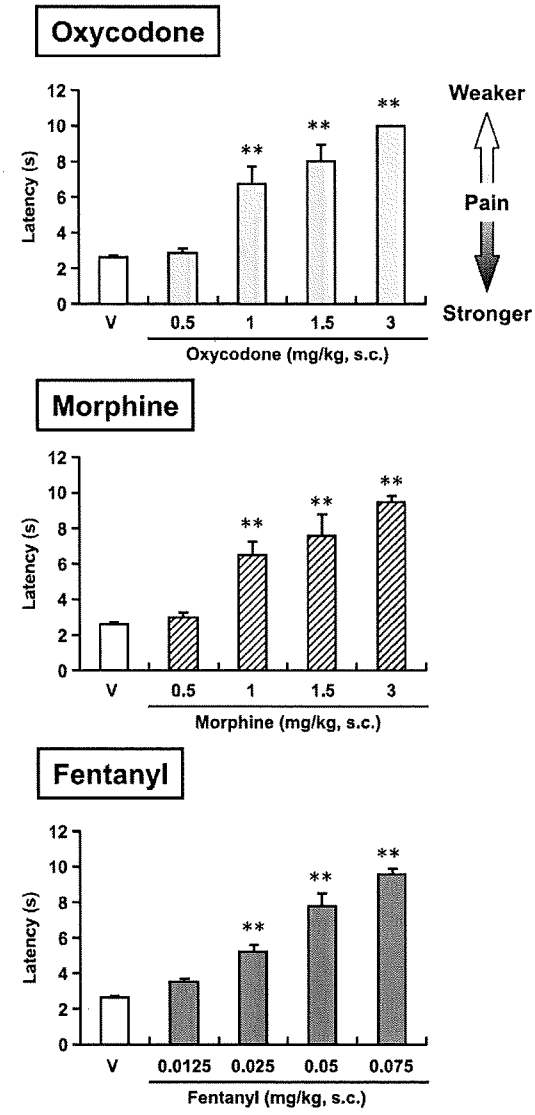

Fig. 7. The effects of oxycodone, morphine, and fentanyl on thermal nociception. The antinociceptive effects of oxycodone, morphine, and fentanyl on thermal nociception in intact ICR mice were evaluated using the tail-flick test. Each opioid was administered subcutaneously 30 min before the measurement. The cut-off time was set at 10 s in the test to avoid injury to the tail. The columns and vertical bars show the means ± S.E.M. (n = 6). $^{**}P<0.01$, compared with the vehicle (V) group (one-way ANOVA and Dunnett's test).

model mice. Oxycodone (2 and 5 mg/kg, s.c.) significantly reversed the decreased withdrawal threshold induced by physical ligation of the sciatic nerve. The strongest analgesic effect (approximately 80% of reversal) occurred with the 5-mg/kg dose, which did not affect the paw withdrawal threshold in the sham-treated group (Fig. 6). Although morphine (20 mg/kg, s.c.) and fentanyl (0.1 and 0.2 mg/kg, s.c.) also reversed the decreased withdrawal threshold in the experimental group, the high doses required were close to or at the doses that significantly affected the withdrawal threshold in the sham-treated group (Fig. 6). These results suggest

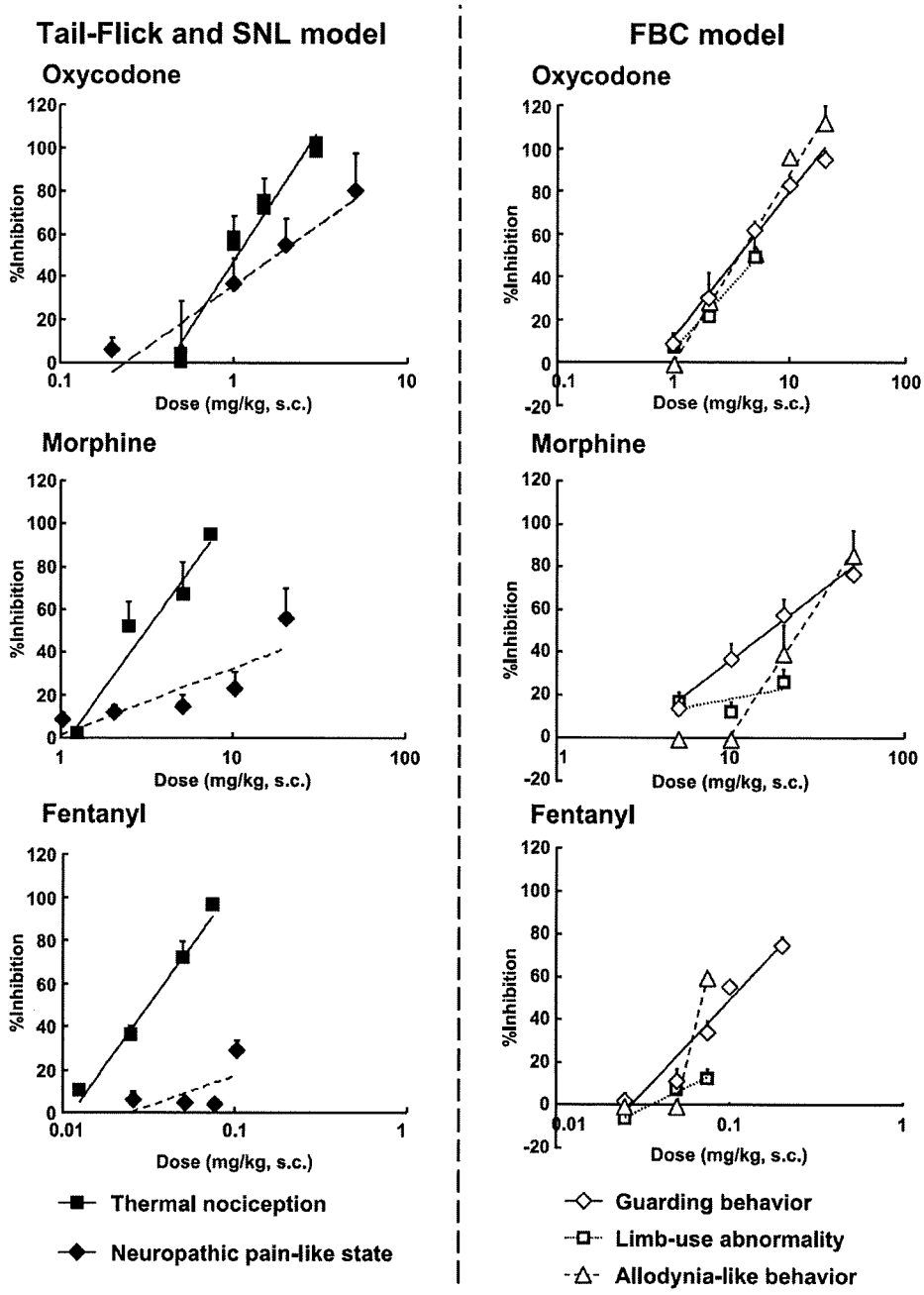

Fig. 8. The linear correlation between dose and percentage inhibition in each opioid obtained from the different pain models. Only the doses that did not affect the sham-treated group were included. Solid and broken lines show the linear correlations between dose and percentage inhibition for oxycodone, morphine, and fentanyl. The left side of the figure indicates the regression lines to thermal nociception in the tail-flick test (filled square) and neuropathic pain-like state in the SNL model (filled diamond). The right side indicates the regression lines to guarding behavior (open diamond), limb-use abnormality (open square), and allodynia-like behavior (open triangle) in the FBC model. The points and vertical bars show the means ± S.E.M. (n = 6 – 8). Right panels: Modified from Ref. 37 (proceeding for The Fourth Asia Pacific Symposium on Pain Control, Kuala Lumpur, November 2 – 4, 2007) with permission from S. Karger AG, Basel.

that among the three opioids, oxycodone has the most favorable pharmacological profile for the treatment of the neuropathic pain–like state in this model.

Effects of oxycodone, morphine, and fentanyl on thermal nociception in mice

To evaluate the antinociceptive effects of oxycodone, morphine, and fentanyl on thermal nociception, the tail-

Table 2. The ED_{50} values of oxycodone, morphine, and fentanyl for thermal nociception, neuropathic pain-like state, guarding behavior, limb-use abnormality, and allodynia-like behavior

	ED_{50} (mg/kg, s.c.) (95% Confidence limits)		
	Oxycodone	Morphine	Fentanyl
Thermal nociception			
ICR mice	0.91 (0.52 – 1.59)	3.00 (1.66 – 5.42)	0.031 (0.020 – 0.048)
Neuropathic-like state (SNL model)			
	1.8 (1.00 – 4.01)	>10	>0.1
Bone cancer pain (FBC model)			
Guarding behavior	5.96 (4.60 – 7.22)	23.6 (18.4 – 29.3)	0.122 (0.113 – 0.134)
Limb-use abnormality	5.04 (4.23 – 6.52)	>20	>0.1
Allodynia-like behavior	6.13 (4.22 – 7.86)	30.6 (24.5 – 37.9)	0.071 (0.070 – 0.071)

The ED_{50} values of oxycodone, morphine, and fentanyl for ongoing, ambulatory, and neuropathic pains were calculated from the regression equations of the regression lines (Fig. 8).

flick latency was measured in ICR mice. Oxycodone (1 – 3 mg/kg, s.c.), morphine (2.5 – 7.5 mg/kg, s.c.), and fentanyl (0.025 – 0.075 mg/kg, s.c.) significantly increased the tail-flick latency in a dose-dependent manner (Fig. 7). To test whether the relative efficacies of the opioids are affected by the genetic background of the model mice, the same experiment was repeated in C3H/HeN mice, which were used to develop the FBC model. Virtually no differences in the effective doses or relative efficacies of the three opioids were observed between the two mouse strains (data not shown). These results show that oxycodone, morphine, and fentanyl are all effective in relieving thermal nociception.

Comparison of the ED_{50} values of oxycodone, morphine, and fentanyl for relieving several types of pain

To compare the equivalent dose-ratios of oxycodone, morphine, and fentanyl, the regression lines of the dose–response relationships for the antinociceptive effects of the three opioids in the mouse pain models were compared. In drawing the regression lines, we excluded the doses that affected behavior in the sham-treated group (Fig. 8) because the behavioral measurements at such doses may reflect not only the antinociceptive effect but also an effect on general behavior. Table 2 shows the ED_{50} values calculated from the regression equations. The ED_{50} values of oxycodone, morphine, and fentanyl for anti-thermal nociception were 0.91, 3.00, and 0.031 mg/kg, respectively. The equivalent dose-ratio is consistent with the previous results reported by others (18). In the SNL model, the ED_{50} value of oxycodone was approximately 2-fold that for anti-thermal nociception. However, the ED_{50} values of morphine and fentanyl could not be calculated in this model because these two opioids did not exhibit at least a 50% reversal of pain-related effects without affecting the behavior of the sham-treated group. In the FBC model, the ED_{50} value of oxycodone was similar among the three different pain behaviors and was approximately 6-fold that for anti-thermal nociception. The ED_{50} values of fentanyl determined by guarding and allodynia-like behaviors were approximately 2- to 4-fold the ED_{50} value of fentanyl for anti-thermal nociception. The ED_{50} values of morphine based on guarding and allodynia-like behaviors were 8- to 10-fold the ED_{50} value of morphine for anti-thermal nociception. However, the ED_{50} values of fentanyl and morphine could not be calculated based on the limb-use abnormality assessment because an adverse effect was observed in the sham group before reaching 50% pain reversal. These results demonstrate that the three opioids have different analgesic efficacies depending on the pain model examined. Among the three opioids, oxycodone appeared to exhibit a preferable pharmacological profile compared with the other two opioids, especially in the SNL and the FBC models.

Discussion

In the present study, the efficacy profiles of oxycodone, morphine, and fentanyl were examined in three mouse pain models. These μ-opioid receptor agonists were found to exhibit different antinociceptive effects in

the FBC and the SNL models. Oxycodone reversed all types of pain examined in the three mouse pain models, whereas morphine and fentanyl were less effective on the ambulatory pain in the FBC model and the neuropathic pain-like state in the SNL model. Thus, oxycodone appears to have distinct analgesic effects compared with the other two opioids.

We employed the FBC model to examine opioid efficacy on bone cancer–related pain in this study. The FBC model was useful as a bone cancer pain model because pain and the pathological changes including bone destruction and nerve compression (21, 24 – 26) were observed within a relatively short period of time (within a few weeks) after implantation of the tumor cells (Fig. 1) (21, 24 – 27), and those were similar to some of the symptoms observed in bone cancer patients. For example, bone cancer patients typically report numbness in the beginning, but the pain becomes severe as the disease progresses, eventually resulting in bone destruction (28, 29). In the FBC model, allodynia-like behavior began within a week after tumor implantation when bone destruction had not yet been observed (Figs. 1 and 2). In the late phase (e.g., within 7 – 14 days), guarding behavior and limb-use abnormality were observed, accompanied by bone destruction, suggesting that the FBC model mimics some of the clinical features observed in human bone cancer pain. In this model, oxycodone exhibited antinociceptive effects on all three types of pain: ongoing, ambulatory, and allodynia-like. On the other hand, neither morphine nor fentanyl exhibited antinociceptive effects on limb-use abnormality without affecting the sham-treated groups. Thus, oxycodone has a preferable overall efficacy profile in this bone cancer pain model.

Since the behavioral changes such as guarding behavior and limb-use abnormality were used to evaluate the efficacy of the opioids, it is possible that the opioid-induced hyperlocomotion might influence the behavioral evaluations in the FBC model. In fact, we found that subcutaneous administration of all three opioids (morphine at 20 mg/kg, oxycodone at 10 mg/kg, fentanyl at 0.1 mg/kg) increased spontaneous activity approximately 2-fold (data not shown). However, the opioid treatments in this study did not affect the functional aspect of the behaviors because no abnormality was observed in the motor function after these opioid treatments even at the highest doses used in the Rota-rod test (morphine at 50 mg/kg, s.c.; oxycodone at 20 mg /kg, s.c.; fentanyl at 0.2 mg/kg, s.c.) (data not shown). Nevertheless the effect of each opioid on the guarding behavior and the limb-use abnormality differed, indicating that the distinctive pharmacological profiles, rather than the general opioid-induced hyperlocomotion, account for the different efficacy in the FBC models.

Neuropathic pain is another clinical situation that does not often respond effectively to opioids. Recently, several clinical reports have shown that oxycodone was effective in controlling neuropathic pain related to DNP and PHN (15, 16). In the present study, we tested the efficacy of the opioids in the animal pain model showing neuropathic pain-like behavior. Among the three opioids, oxycodone exhibited greater antinociceptive effects on allodynia-like behavior in the FBC model and on the neuropathic pain-like state in the SNL model within a dose range that did not affect the sham group. These results suggest that oxycodone may possess distinct pharmacological profiles in the treatment for some types of neuropathic pain.

In contrast to the efficacy in the FBC and the SNL models, all three opioids displayed antinociceptive effects on thermal nociception in the tail-flick test, which has been commonly used to evaluate the efficacy of many drugs including opioids. The equivalent dose-ratio calculated from the ED_{50} values of oxycodone, morphine, and fentanyl was approximately 1:3:0.03, which is similar to the previously reported ratio (18). On the other hand, the equivalent dose-ratio was changed when these opioids were tested in other types of pain, showing that the efficacy profiles of those opioids differ depending on the types of pain to control. It is important to understand the efficacy profile of each opioid for appropriate opioid use.

In the present study, we used relatively high doses of the opioids. Although it is difficult to speculate whether the doses used in the present study are clinically relevant, the plasma concentration after the subcutaneous injection of morphine at 5 mg/kg and oxycodone at 2 mg/kg in mice were similar to those after oral administration of 300 mg/day of morphine and 120 mg/day of oxycodone in humans, respectively. This may suggest that the opioid doses used in our studies were not far different from the clinically used dose-ranges to manage cancer-related severe pain (14, 30). However, this kind of analysis may not be appropriate, and special care is needed to compare our animal study to the clinical setting. In the meanwhile, it is noteworthy that some recent papers showed that the clinical doses of oxycodone were effective for relieving pain in patients suffering from bone metastasis or neural injury (15, 16, 31).

One other interpretation of our results in the FBC model is that the opioid treatments might have rapidly inhibited tumor growth, so that pain intensity was alleviated as a result of reduced tumor size in the bone rather than an antinociceptive effect. Therefore, the effect of each opioid on the size of the implanted tumor in the FBC model mice was tested by using a bio-

luminescent imaging system. None of the opioid treatments inhibited the tumor size at 30 min or 24 h after drug administration (data not shown), showing that a change in tumor size did not contribute to the observed analgesic effect of oxycodone, morphine, or fentanyl.

Nielsen et al. (32) previously reported that the antinociceptive effect of oxycodone is mediated by the κ-opioid receptor. One could assume, therefore, that the difference in the efficacy profiles among the opioids may originate from a difference in the activated receptors and that the κ-opioid receptor as well as the μ-opioid receptor may mediate the effects of oxycodone, resulting in better drug efficacy. Our preliminary data, however, suggested that the antinociceptive effects of all three opioids in the FBC model were completely antagonized by a μ-opioid receptor antagonist, β-FNA, and not by a κ-opioid receptor antagonist, nor-BNI (K. Minami et al., in preparation). Therefore, the μ-opioid receptors appeared to mediate the analgesic effects of all three opioids.

Currently no data is available to explain the observed difference in the pharmacological profiles among these three opioids. There are, however, several possible hypotheses. For example, it has been reported that several receptors are known to couple to multiple effecters to initiate downstream signals and that different ligands can promote distinct relative efficacies in the downstream signals, resulting in a ligand-dependent efficacy profile (33). Another possibility is that different types of the μ-opioid receptor splice variants are responsible for different efficacy of each opioid. Several μ-opioid receptor splice variants have been identified (34), and it is possible that each splice variant may utilize a different downstream signaling pathway or are expressed in different anatomical regions to exhibit a distinctive pharmacological profile. Moreover, heterodimerization of the μ-opioid receptor and other receptors is another possible mechanism for the different opioid efficacy since the intracellular signals including a coupled G-protein can be affected by receptor dimerization (35, 36). Additional experiments are required to verify these hypotheses.

In conclusion, the present study showed that oxycodone produced the most distinguished antinociceptive effects on the FBC and SNL models. The analgesic effects of all three opioids are suggested to be mediated via μ-opioid receptors. It is of great interest to investigate the underlying mechanisms of the different efficacies among these μ-opioid agonists.

Acknowledgments

The authors thank Dr. Donald J. Kyle (Purdue Pharma L.P., Cranbury, NJ, USA) for his expert comments on this manuscript. There is no conflict of interest, including financial support, with Purdue Pharma L.P. regarding this research.

References

1 Moulin DE, Iezzi A, Amireh R, Sharpe WKJ, Boyd D, Merskey H. Randomised trial of oral morphine for chronic non-cancer pain. Lancet. 1996;347:143–147.
2 Cherny NI, Thaler HT, Friedlander-Klar H, Lapin J, Foley KM, Houde R, et al. Opioid responsiveness of cancer pain syndromes caused by neuropathic pain or nociceptive mechanisms: a combined analysis of controlled single-dose studies. Neurology. 1994;44:857–861.
3 Watson CP, Watt-Watson JH. Treatment of neuropathic pain: focus on antidepressants, opioids and gabapentin. Pain Res Manage. 1999;4:168–178.
4 Smith T, Robert AN. Review of duloxetine in the management of diabetic peripheral neuropathic pain. Vasc Health Risk Manage. 2007;3:833–844.
5 Becker R, Jakob D, Uhle EI, Riegel T, Bertalanffy H. The significance of intrathecal opioid therapy for the treatment of neuropathic cancer pain conditions. Stereotact Funct Neurosug. 2000;75:16–26.
6 Mercadante S, Arcuri E. Breakthrough pain in cancer patients: pathophysiology and treatment. Cancer Treat Rev. 1998;24:425–432.
7 Portenoy RK, Payne D, Jacobsen P. Breakthrough pain: characteristics and impact in patients with cancer pain. Pain. 1999;81:129–134.
8 Cherny N. New strategies in opioid therapy for cancer pain. J Oncol Manage. 2000;9:8–15.
9 Hanks GW, Conno F, Cherny N, Hanna M, Kalso E, McQuay HJ, et al. Expert Working Group of the Research Network of the European Association for Paliative C. Morphine and alternative opioids in cancer pain: the EAPC recommendations. Br J Cancer. 2001;84:587–593.
10 Mercadante S. Malignant bone pain: pathophysiology and treatment. Pain. 1997;69:1–18.
11 World Health Organization. Cancer pain relief. Geneva: World Health Organization; 1986.
12 World Health Organization. Cancer pain relief, 2nd ed. Geneva: World Health Organization; 1986.
13 Kalso E. Oxycodone. J Pain Symptom Manage. 2005;29:S47–S56.
14 Bercovitch M, Adunsky A. High dose controlled-release oxycodone in hospice care. J Pain Palliat Care Pharmacother. 2006;20:33–39.
15 Watson CPN, Babul N. Efficacy of oxycodone in neuropathic pain. A randomized trial in postherpetic neuralgia. Neurology. 1998;50:1837–1841.
16 Watson CPN, Moulin D, Watt-Watson J, Gordon A, Eisenhoffer J. Controlled-release oxycodone relieves neuropathic pain: a randomized controlled trial in painful diabetic neuropathy. Pain. 2003;105:71–78.
17 Narita M, Nakamura A, Ozaki M, Imai S, Miyoshi K, Suzuki M, et al. Comparative pharmacological profiles of morphine and oxycodone under a neuropathic pain like state in mice: evidence for less sensitivity to morphine. Neuropsychopharmacology. 2007;33:1097–1112.

18 Lemberg K, Kontinen VK, Viljakka K, Kylänlahti I, Yli-Kauhaluoma J, Kalso E. Morphine, oxycodone, methadone and its enantiomers in different models of nociception in the rat. Anesth Analg. 2006;102:1768–1774.
19 El Mouedden M, Meert TF. Evaluation of pain-related behavior, bone destruction and effectiveness of fentanyl, sufentanil, and morphine in a murine model of cancer pain. Pharmacol Biochem Behav. 2005;82:109–119.
20 Honore P, Lugar NM, Sabino MAC, Schwei MJ, Rogers SD, Mach DB, et al. Osteoprotegerin blocks bone cancer-induced skeletal destruction, skeletal pain and pain-related neurochemical reorganization of the spinal cord. Nat Med. 2000;6: 521–528.
21 Luger NM, Sabino MA, Schwei MJ, Mach DB, Pomonis JD, Keyser CP, et al. Efficacy of systemic morphine suggests a fundamental difference in the mechanisms that generate bone cancer vs. inflammatory pain. Pain. 2002;99:397–406.
22 Zhao C, Chen L, Tao YX, Tall JM, Borzan J, RingKamp M, et al. Lumbar sympathectomy attenuates cold allodynia but not mechanical allodynia and hyperalgesia in rats with spared nerve injury. J Pain. 2007;8:931–937.
23 Narita M, Nakajima M, Miyoshi K, Narita M, Nagumo Y, Miyatake M, et al. Role of spinal voltage-dependent calcium channel $\alpha 2\delta$-1 subunit in the expression of a neuropathic pain-like state in mice. Life Sci. 2007;80:2015–2024.
24 Vermeirsch H, Nuydens RM, Salmon PL, Meert TF. Bone cancer pain model in mice: evaluation of pain behavior, bone destruction and morphine sensitivity. Pharmacol Biochem Behav. 2004;79:243–251.
25 Gilchrist LS, Cain DM, Harding-Rose C, Kov AN, Wendelschafer-Crabb G, Kennedy WR, et al. Re-organization of P2X3 receptor localization on epidermal nerve fivers in a murine model of cancer pain. Brain Res. 2005;1044:197–205.
26 Peters CM, Ghilardi JR, Keyser CP, Kubota K, Lindsay TH, Lugar NM, et al. Tumor-induced injury of primary afferent sensory nerve fivers in bone cancer pain. Exp Neurol. 2005;193: 85–100.
27 Sevcik MA, Ghilardi JR, Peters CM, Limdsay TH, Halvorson KG, Jonas BM, et al. Anti-NGF therapy profoundly reduces bone caner pain and the accompanying increase in markers of peripheral and central sensitization. Pain. 2005;115:128–141.
28 Komiya S, Zenmyo M, Inoue A. Bone tumors in the pelvis presenting growth during pregnancy. Arch Orthop Trauma Surg. 1999;119:22–29.
29 Pandit-Taskar N, Batraki M, Divgi CR. Radiopharmaceutical therapy for palliation of bone pain from opsseous metastases. J Nucl Med. 2004;45:1358–1365.
30 Kirou-Mauro AM, Hird A, Wong J, Sinclair E, Barnes EA, Tsao M. Has pain management in cancer patients with bone metastases improved? A seven-year review at an outpatient palliative radiotherapy clinic. J Pain Symptom Manage. 2009; 37:77–84.
31 Hara S. Opioids for metastatic bone pain. Oncology. 2008;74 Suppl 1:52–54.
32 Nielsen CK, Ross FB, Lotfipour S, Saini KS, Edwards SR, Smith MT. Oxycodone and morphine have distinctly different pharmacological profiles: radioligand binding and behavioural studies in two rat models of neuropathic pain. Pain. 2007; 132:289–300.
33 Galandrin S, Oligny-Longpre G, Bouvier M. The evasive nature of drug efficacy: implications for drug discovery. Trends Pharmacol Sci. 2007;28:423–430.
34 Pan YX, Xu J, Moskowitz HS, Xu M, Pasternak GW. Identification of four novel exon 5 splice variants of the mouse μ-opioid receptor gene: functional consequences of C-terminal splicing. Mol Pharmacol. 2005;68:866–875.
35 Hojo M, Sudo Y, Ando Y, Minami K, Takada M, Matubara T, et al. μ-Opioid receptor forms a functional heterodimer with cannabinoid CB1 receptor: electrophysiological and FRET assay analysis. J Pharmacol Sci. 2008;108:308–319.
36 Hasbi A, Nguyen T, Fan T, Cheng R, Rashid A, Alijaniaram A, et al. Trafficking of preassembled opioid μ-δ heterooligomer-Giz signaling complexes to the plasma membrane: coregulation by agonists. Biochemistry. 2007;46:12997–13009.
37 Kato A, Minami K, Ito H, Tomii T, Matsumoto M, Orita S, et al. Oxycodone-induced analgesic effects in bone cancer pain model in mice. Oncology. 2008;74 Suppl 1:55–60.

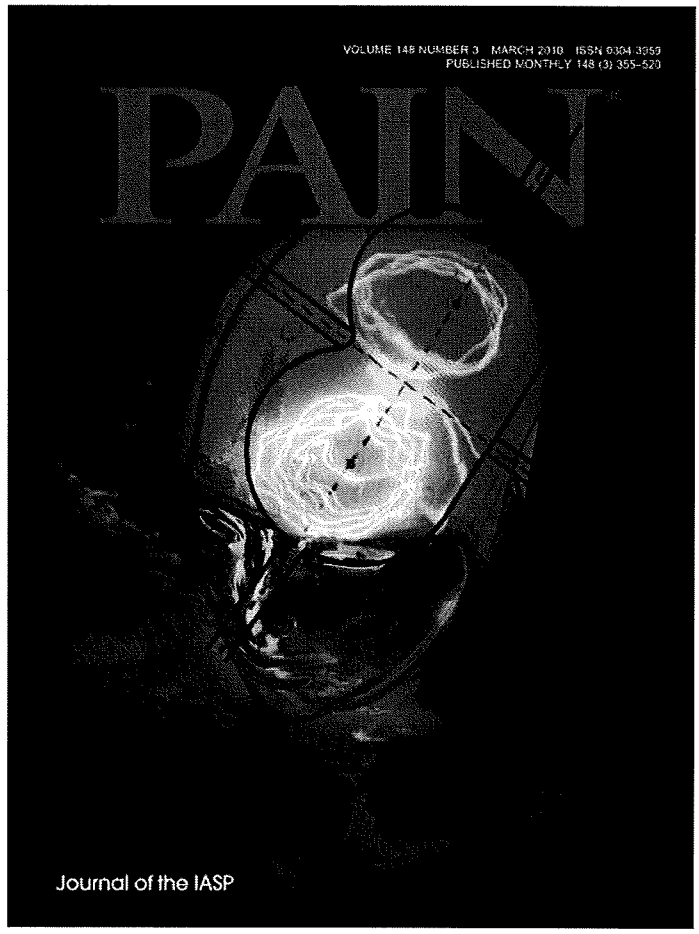

PAIN® 148 (2010) 426–430

PAIN®

www.elsevier.com/locate/pain

Comparison of pain and dyspnea perceptual responses in healthy subjects

Takashi Nishino *, Eiko Yashiro, Hisanori Yogo, Shiroh Isono, Norihiro Shinozuka, Teruhiko Ishikawa

Department of Anesthesiology, Graduate School of Medicine Chiba University, 1-8-1 Inohanacho, Chiba 260-8670, Japan

ARTICLE INFO

Article history:
Received 30 May 2009
Received in revised form 6 November 2009
Accepted 30 November 2009

Keywords:
Breathholding test
Cold-pressor test
Dyspnea
Pain

ABSTRACT

Dyspnea and pain have a number of similarities. Recent brain imaging experiments showed that similar cortical regions are activated by the perceptions of dyspnea and pain. We tested the hypothesis that an individual's pain sensitivity might parallel the individual's dyspnea sensitivity. Studies were carried out in 52 young healthy subjects. Each subject experienced experimentally induced pain and dyspnea. Pain was induced by a cold-pressor test and dyspnea was induced by breathholding while the unpleasant experience of pain and dyspnea was assessed by using a Visual Analogue Scale (VAS). The times from the start of cold stimulation and breathholding to the onset of uncomfortable sensation (pain threshold time and the period of no respiratory sensation, respectively) and to the limit of tolerance (pain endurance time and total breathholding time, respectively) were also measured. In response to cold pain stimulation, a behavioral dichotomy (pain-tolerant and pain-sensitive) was observed. The period of no respiratory sensation was significantly shorter in the PS (pain-sensitive) group than in the PT (pain-tolerant) group (16.9 ± 3.8 vs. 19.6 ± 5.3 s: $P < 0.05$), whereas no significant difference in the total breathholding time was found between the PT and PS groups. A significant correlation was observed between the pain threshold time and the period of no respiratory sensation in both the PT and PS groups. However, no significant association was observed between pain and dyspnea tolerance in both groups. In conclusion, an individual's pain threshold is correlated to the individual's dyspnea threshold, but the individual's pain tolerance is not consistently correlated to the individual's dyspnea tolerance.

1. Introduction

Although dyspnea and pain are distinctly different sensations, dyspnea shares many clinical, physiological, and psychological features with pain [9,13]. Both pain and dyspnea are not only alarming signs but also uncomfortable sensations that contain an affective as well as a sensory dimension [13]. Considering the analogies between pain and dyspnea, it is quite conceivable that there may be some neurophysiological link between pain and dyspnea. In fact, recent brain imaging studies have shown that very similar cortical regions are activated by the perceptions of pain and dyspnea [1,8,14,20,21,30,31]. Also, data available from studies in the same subjects strongly suggest that dyspnea and pain activate the common neurophysiological pathways. For example, the study of Morélot-Panzini et al. [16] showed that there is a neurophysiological connection between pain and dyspnea. In addition, the recent study by von Leupoldt et al. [32] showed that the perceived unpleasantness of resistive load-induced dyspnea is processed in the human anterior insula and amydala, the activation of which has been implicated in the affective processing of pain [23].

The study of Chen et al. [6] showed that there are two groups of normal healthy subjects whose responses to cold pain stimulation are quite different, i.e., pain-sensitive (PS) and pain-tolerant (PT) subjects. The dyspnea sensitivity in these different groups of subjects has never been investigated. Assuming that pain and dyspnea share common neurophysiological pathways/areas such as the spinothalamic pathway, cortico-limbic somatosensory pathway, insular cortex, and cingulate cortex, it is possible that individuals having a high sensitivity for pain may also have a high sensitivity for dyspnea. To test this hypothesis, we conducted experiments in which healthy subjects performed maximal breathholding and cold-pressor tests while assessing their uncomfortable sensation using a visual analogue scale (VAS).

2. Methods

2.1. Subjects

The study protocol was approved by the Institutional Ethical Committee of Chiba University (Chiba, Japan), which conforms to the standard set by the Declaration of Helsinki (2000) of the World Medical Association. Studies were carried out in 52 young healthy subjects (33 males and 19 females), whose ages ranged from 22 to 33 yr. None had clinical evidence of respiratory, cardiovascular,

* Corresponding author. Tel.: +81 43 226 2155; fax: +81 43 226 2156.
E-mail address: nishinot@faculty.chiba-u.jp (T. Nishino).

0304-3959/$36.00
doi:10.1016/j.pain.2009.11.024

neurological or neuromuscular disorders. Each subject gave an informed consent to the methodology of the study. None was a smoker or was aware of the hypothesis tested in the studies. Mean heights and weights of male subjects were 173.9 + 6.2 cm and 65.4 + 8.0 kg (mean + SD), respectively, and the mean values in female subjects were 160.2 + 6.3 cm and 50.2 + 3.6 kg, respectively.

2.2. Instruments

The subjects were tested in the sitting posture in an air-conditioned, temperature (24–25 °C) controlled room. Skin temperature was measured using a temperature sensor (Mon-a-therm Skin Probe, Tyco Healthcare Group LP, Tokyo, Japan) taped securely on the back of the subject's left hand. Pain was induced by a cold-pressor test. The left hand of each subject was immersed up to the wrist in ice water (0–1 °C), palm down on the bottom of the ice-water container. Local skin adaptation was prevented by stirring the ice water. The subject was asked to keep her/his hand in the ice water as long as possible, or to the cut-off limit of 3 min was reached. During the immersion of the left hand in the ice water, the subject was asked to rate continuously the sensation of pain by using a visual analogue scale (pain VAS). The analogue scale consisted of a horizontal 10 cm line with equally spaced markers. The subject could control the position of the knob of the linear potentiometer along this line. The numerical value of zero indicated "no discomfort at all", 100 indicated a sensation that was "intolerable discomfort". The subject was instructed that he or she could remove the hand any time prior to 3 min if pain was intolerable or the VAS value reached 100. Immediately after completion of the cold water test run, all the subjects put their hand into the warm water box (38 °C).

In order to conduct dyspnea experiments, the subjects breathed through an experimental apparatus containing a face mask, a pneumotachograph, and a one-way valve system. Details of the experimental setup are given elsewhere [19]. In brief, ventilatory airflow, tidal volume (V_T), mask pressure (P_{mask}), and end-tidal carbon dioxide tension ($P_{ET}CO_2$) were continuously measured. Dyspneic sensation was induced by breathholding. Each subject was asked to rate continuously the intensity of the sensation of dyspnea, which was defined as the sensation of respiratory discomfort by using the aforementioned visual analogue scale (dyspneic VAS, 0: no discomfort at all; 100: intolerable discomfort). The onset of dyspnea/pain was identified by a sudden rise in dyspneic VAS above 0.

2.3. Experimental protocol

The subjects were given a short training period to accustom them to the use of the VAS for both pain and dyspnea. In each subject, the cold-pressor test was conducted first. Then, the subject wore the respiratory experimental apparatus. When all the respiratory variables were stable while breathing room air (baseline condition), the breathholding test was conducted. Instructions were given that the sensation felt during the baseline period was equivalent to "0." No further instruction was given. The subject was asked to stop breathing at end-expiration (assessed by expiratory flow and plateaued $P_{ET}CO_2$ traces) and to hold his or her breath for as along as possible while rating continuously the sensation of dyspnea.

2.4. Data analysis

Pain threshold time (PTT) was defined as the time from immersion of the hand in the ice water to the onset of pain sensation (Fig. 1). Pain endurance time (PET) is the duration from the ice water immersion of subject's hand until the withdrawal of the hand. Skin surface temperature at the threshold and the withdrawal were also obtained. When the subject reached the cut-off time of 3 min, the pain endurance duration was recorded as 180 s and the maximal value of pain VAS before the cut-off time was obtained. Subjects who reached the cut-off time were designated "pain-tolerant (PT)" and those subjects who withdrew their hands before the cut-off time were designated "pain-sensitive (PS)".

Before the breathholding test, values of respiratory variables during the baseline were obtained from recording of the 1 min of resting breathing. Minute ventilation (V_I) is defined as the product of V_T and respiratory frequency. During the breathholding test, the period of no respiratory sensation (NRS) was defined as the time from the start of breathholding to the onset of unpleasant sensation and the total breathholding time (BHT) was defined as the time from the start of breathholding to the breaking point (dyspneic VAS = 100) (Fig 2).

A sample size calculation was based on the results of our preliminary study in which the relationship between PTT and NRS period was analyzed in 6 subjects. For a correlation coefficient value of 0.4 and 0.05 level of significance test with at least 80% power, the sample size of 48 would be adequately powered to detect a statistically significant result.

The data were expressed as mean ± SD, and statistical analysis was performed by the use of a parametric analysis (one way repeated measures of analysis of variance and unpaired t-test) when normality had passed. Some data which failed normality were analyzed by a non-parametric test (Mann–Whitney rank sum test). The association between two variables representing threshold and tolerance was quantified by using the Pearson product moment–correlation test. All analyses were performed with the statis-

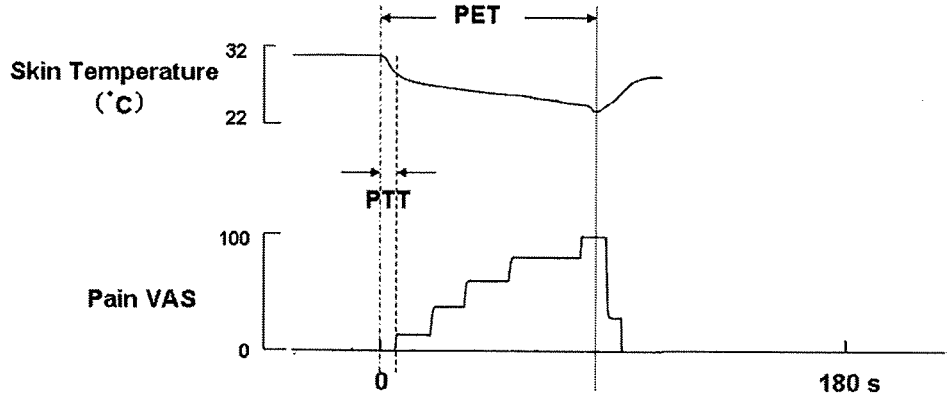

Fig. 1. Changes in skin temperature and pain VAS during immersion of the hand in the ice-water. Definitions of pain threshold time (PTT) and pain endurance time (PET) are shown.

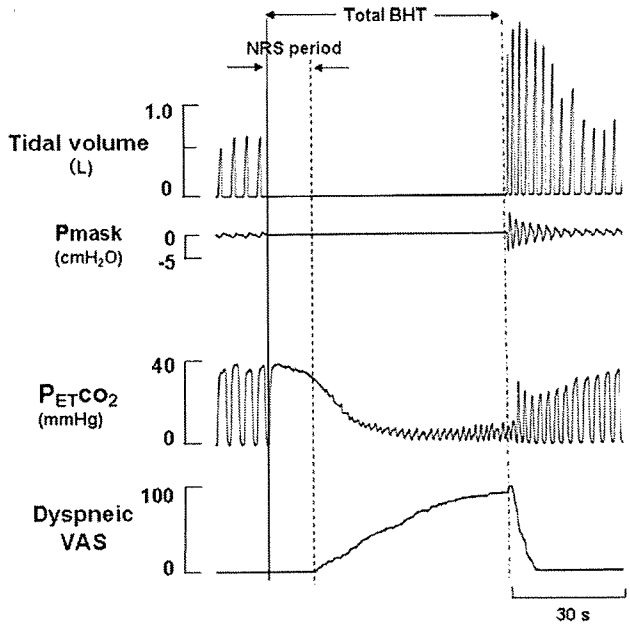

Fig. 2. Changes in dyspnea VAS during breathholding. Solid line, dash line, and dash-dot line indicate the start of breathholding, the onset of dyspnea, and the breaking point of breathholding, respectively. Definitions of the period of no respiratory sensation (NRS) and total breathholding time (BHT) are also shown.

tical package SigmaStat (SigmaStat 3.0, SPSS Inc., Chicago, IL). $P < 0.05$ was considered significant.

3. Results

In response to immersion of the subjects' hands in the ice water, all subjects started to feel pain within 30 s. Of the total 52 subjects, 25 subjects tolerated the cold-pressor-induced pain for 180 s whereas 27 subjects could not tolerate and withdrew their hands from ice water before the cut-off time of 3 min. Twenty-six of these subjects withdrew after 100 s or less.

Based on these dichotomized responses, our subjects were clearly divided into two groups, i.e., PT and PS groups. Specific information regarding the two groups during pain-induced and breathholding tests are listed in Table 1.

Threshold. The values of no respiratory sensation period in the PS group were slightly but significantly shorter than those in the PT group. Fig. 3 shows the relationship between the pain threshold time and the period of no respiratory sensation. A significant correlation was observed between the two threshold variables in each group and also across both groups.

Tolerance. The mean breathholding time was nearly identical in the PS and PT groups. No significant difference was observed.

Since the ceiling effect observed during the cold-pressor test reduces effectiveness of the correlation procedure, the relationship between dyspnea tolerance (total breathholding time) and pain tolerance was analyzed by employing different variables associated with pain tolerance, i.e., pain endurance time in the PS group and maximal pain VAS in the PT group. In these analyses, a significant association was observed neither between the pain endurance time and the total breathholding time in the PS group (Fig. 4a) nor between the maximal pain VAS and the total breathholding time in the PT group (Fig. 4b).

Comparison between male and female subjects revealed that there was no significant difference in pain and dyspnea variables except that there was a significant difference in maximal breathholding time between males and females (males: 52.3 ± 18.5 vs. females: 41.9 ± 18.6 s, $P < 0.05$).

Table 1
Group characteristics and changes in pain and respiratory parameters during cold-pressor-induced and breathholding tests.

Group	PT	PS
Total No.	25	27
Male/female ratio	19/6	14/13
Skin temperature (°C)		
Control	31.5 ± 1.3	31.5 ± 1.1
Threshold	28.6 ± 1.7	28.8 ± 1.7
Withdrawal	19.4 ± 2.1	23.8 ± 1.9#
Pain threshold time (s)	12.2 ± 5.8	7.7 ± 3.2#
Pain endurance time (s)	180	62.1 ± 28.0#
Maximal pain VAS	78.3 ± 13.1	100*
No respiratory sensation period (s)	19.6 ± 5.3	16.9 ± 3.8*
Total breathholding time (s)	48.2 ± 15.8	48.8 ± 21.9
Baseline breathing		
V_T (L)	0.65 ± 0.11	0.65 ± 0.12
R_f (bpm)	13.6 ± 2.9	13.3 ± 2.8
V_I (L/min)	8.8 ± 1.9	8.5 ± 1.7
$P_{ET}CO_2$ (mmHg)	39.9 ± 2.8	39.1 ± 2.2

PT, pain-tolerant; PS, pain-sensitive.
V_T, tidal volume; R_f, respiratory frequency; V_I, minute ventilation; $P_{ET}CO_2$, end-tidal PCO_2.
* $P < 0.05$, compared with PT- group.
# $P < 0.01$, compared with PT- group.

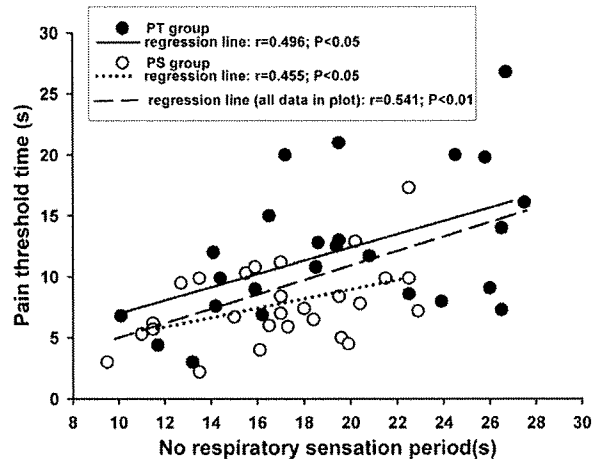

Fig. 3. Relationship between pain threshold time and no respiratory sensation period.

4. Discussion

The results of our study indicate that individuals having a low threshold for cold-pressor-induced pain have a low threshold for air hunger whereas individuals having a low tolerance for cold-pressor-induced pain do not necessarily have a low tolerance for air hunger.

Threshold and tolerance for pain and dyspnea should not be viewed as simple extremes of sensory scales in sensations of pain and dyspnea. Each of these variables is independently influenced by physiologic and psychological variables that contribute to the neural integrative capacity of the central nervous system to produce individual differences in threshold and tolerance [11]. Recent studies [9,13] suggest that like pain, dyspnea has a sensory-discriminative (intensity) dimension and an affective (unpleasantness) dimension. In this connection, it has been demonstrated that intensity and unpleasantness of pain are processed differently

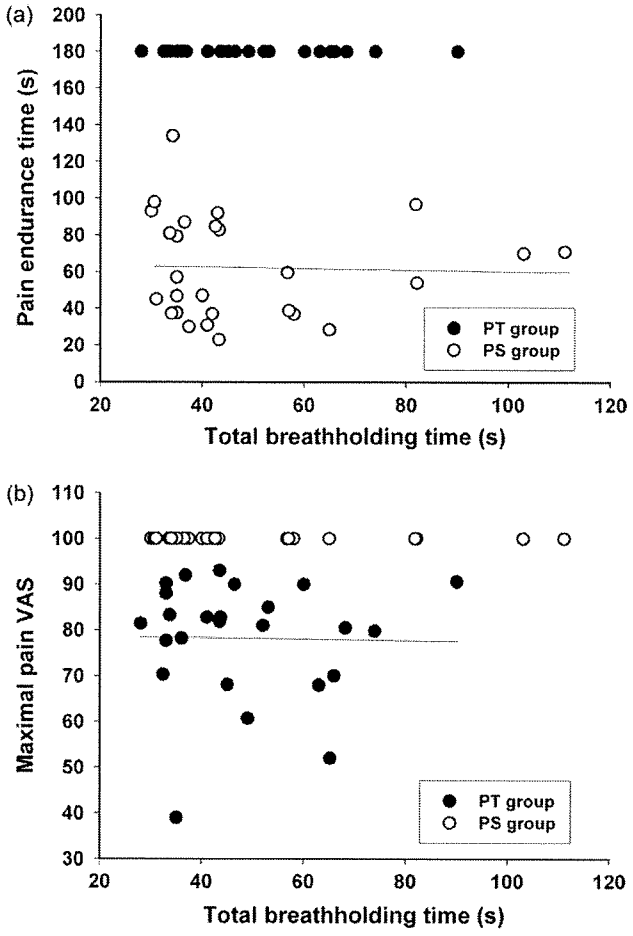

Fig. 4. Relationship between pain and dyspnea tolerance. (a) Relationship between pain endurance time and total breathholding time in the pain-sensitive (PS) group. (b) Relationship between maximal pain VAS and total breathholding time in the pain-tolerant (PT) group.

[17,22], although pain unpleasantness is often closely linked to the intensity of the painful sensation. It is evident that the threshold is closely associated with the sensory-discriminative dimension. Since the tolerance appears to be closely related to behaviors of escape and avoidance, the tolerance may be associated more closely with the affective dimension than the threshold.

Our finding that the pain threshold time was significantly correlated to the period of no respiratory sensation is compatible with the notion that pain and dyspnea would share common neurophysiologic pathways and mechanisms associated with the sensory-discriminative dimensions of pain and dyspnea. However, the finding that the total breathholding time was never correlated to any variables associated with pain tolerance may not be easily reconciled with the above notion. Furthermore, our finding seems to be contrary to the finding of Schön et al. [24] who showed a high correlation between perceived dyspnea and pain in the unpleasantness dimension, but not in the intensity dimension. In the study of Schön et al. [24], healthy subjects were exposed to brief, mild inspiratory loads, which probably produced mainly a sensation of work/effort whereas in our breath-hold study the main sensation produced is the sensation of air hunger. It is also apparent that the prolonged breath-hold caused much higher levels of unpleasantness, compared with the brief, mild inspiratory loads [2]. Although it is not clear how much the methodological discrepancies contribute to the different findings between the two studies, a simple comparison of the finding of Schön et al. [24] and our finding may not be entirely valid.

To explain the lack of correlation between tolerance responses of pain and air hunger observed in this study, several factors influencing pain and/or air hunger have to be considered.

First, the tolerance seems to be more malleable to repeated noxious stimulation as compared with the threshold. In this connection, environmental factors seem to play important roles in characterizing individual's tolerance for pain and air hunger. For example, habituation is a common reaction to both pain [4] and breath-hold [12,18]. In daily life, even healthy human subjects may have repeated experiences of air hunger induced by heavy exercise or they may have repeated exposures to various types of acute and chronic pain. These experiences of air hunger and pain may independently lead the subjects to develop an ability of tolerating an increased level of discomfort. It is quite possible that an individual's pain tolerance may not parallel the individual's air hunger tolerance. The results of recent studies suggest that pain tolerance may be at least partially inherited [5,7], indicating the importance of genetic factors. In addition, there is a report [26] to support a dominant mode of inherence for congenital central alveolar hypoventilation syndrome (CCHS) which is a rare neuropathologic syndrome characterized by a lack of ventilatory response to CO_2 and a lack of air hunger during CO_2 inhalation or during maximal breath-hold [25]. The patients with CCHS need anesthesia for painful surgical procedures [27]. Thus, pain tolerance and air hunger tolerance may be separately and independently influenced not only by acquired factors but also by genetic factors.

Psychological and social factors including anxiety, expectancies, and attitudes may also influence the tolerance of pain and air hunger, and in fact, multidimensional model of dyspnea based on a state-of-the pain model has been proposed to emphasize the importance of these factors in affective responses [13]. Thus, pain tolerance and air hunger tolerance are likely influenced separately by many factors, causing a wide individual variation in the responsiveness of pain and air hunger.

Second, our hypothesis is based on the assumption that air hunger and pain would share common neurophysiological pathways. Recent neuroimaging studies have suggested that the thalamocortical projections to the specific cortical regions may be common to both pain and dyspnea [1,8,14,20,21,30,31]. However, this does not necessarily mean that air hunger and pain share and activate identical neural structures. Rather, it is more likely that a clear differentiation of air hunger and pain exists within the neural pathways. The finding that there is no significant association between pain endurance time and total breathholding time suggests that pain and air hunger may activate slightly different regions in the thalamus and distinct cortical sites or that air hunger and pain may produce differential activation patterns in limbic and paralimbic areas despite the activation of a similar neural network. The above-mentioned notion can be supported by the study of Strigo et al. [28] who showed that two different modalities of pain stimulation not only activate different cortical regions but also produce differential activation patterns within various forebrain structures.

Third, the perception of pain and dyspnea can be modified by the descending control systems, and it is possible that the lack of correlation between pain and dyspnea tolerance in each individual may be due to the difference in the influence from the descending control systems on pain and dyspnea. There are well-characterized anatomical networks that influence transmission of sensory information and produces either inhibition or facilitation of nociceptive processing [10]. For example, the response of nociceptive spinal cord neurons can be inhibited by the stimulation of various supraspinal structures [15]. The inhibitory descending circuit, of which the periaqueductal grey (PAG) is included, is best known and

evokes stimulation-produced analgesia [3]. Also, the PAG has been shown to be a site for higher cortical control of pain modulation in humans [29]. A similarly robust descending dyspnea modulatory system has never been shown, and therefore, the descending neural systems may be much stronger in pain, compared with dyspnea. In this connection, a recent study of von Leupoldt et al. [33] suggests that the PAG may play an important role in a down-regulation of insular cortex responses to dyspnea and pain in asthmatic patients who have repeated dyspnea experiences over the course of the disease.

4.1. Limitations of the study

In this study, we used the cold-pressor test to determine the pain sensitivity for each subject since this test has the advantage of being widely used and safe. However, the cold-pressor test has a methodological disadvantage of ceiling effect. In our study, nearly half of subjects tolerated cold-pressor-induced pain for the period of 3 min (PT group). The test time of the cold-pressor test cannot usefully be extended because the skin becomes numb. In fact, some subjects in the PT group reported the increasing numbness of hand immersed in the ice water with a gradual decrease in pain score after the peak value of pain. Although stronger noxious stimuli for pain might cause the shortening of tolerance time and thereby, more precise analyzes of the pain endurance time might be possible, this may not ethically be allowed. Since this ceiling effect reduces the effectiveness of correlation analysis, we had to use the values of maximal pain VAS instead of pain endurance time to examine the correlation between pain and air hunger tolerance in the PT group. Although the maximal pain VAS is considered to be associated with pain sensitivity and tolerance, the maximal pain VAS is not identical to the pain endurance time. Nonetheless, the lack of correlation between the maximal pain VAS and the total breathholding time in the PT group may be comparable to the lack of correlation between the pain endurance time and the total breathholding time in the PS group. In the present study no differentiation was made between ratings for unpleasantness and intensity of pain/air hunger. We cannot deny the possibility that some subjects might have rated more preferentially the affective aspects while others might have rated the sensory aspects of pain and air hunger, causing large individual differences in tolerance between pain and air hunger. However, the sensation of air hunger during the breath-hold is affective in nature and in addition, it has been shown that the measures of pain intensity and pain aversiveness are highly correlated for the cold-pressor test [6]. Thus, it is less likely that the above possibility may explain the lack of correlation between pain and air hunger tolerance.

In conclusion, an individual's air hunger tolerance is unpredictable from the individual's pain tolerance.

Acknowledgement

The authors state that there are no conflicts of interest regarding this work. This work was supported in part by a grant from the Strategy for Cancer Control from the Ministry of Health, Labour and Welfare of Japan.

References

[1] Banzett RB, Mulnier HE, Murphy K, Rosen SD, Wise RJ, Adams L. Breathlessness in humans activates insular cortex. Neuroreport 2000;11:2117–20.
[2] Banzett RB, Pedersen SH, Schwartzstein RM, Lansing RW. The affective dimension of laboratory dyspnea: air hunger is more unpleasant than work/effort. Am J Respir Crit Care Med 2008;177:1384–90.
[3] Behbehani MM. Functional characteristics of the midbrain periaqueductal gray. Prog Neurobiol 1995;46:575–605.
[4] Bingel U, Schoell E, Herken W, Buchel C, May A. Habituation to painful stimulation involves the antinociceptive system. Pain 2007;131:21–30.
[5] Birklein F, Depmeier C, Rolke R, Hansen C, Rautenstrauss B, Prawitt D, Magerl W. A family-based investigation of cold pain tolerance. Pain 2008;138:111–8.
[6] Chen ACN, Dworkin SF, Haug J, Gehrig J. Human pain responsivity in a tonic pain model: psychological determinants. Pain 1989;37:143–60.
[7] Edwards RR, Fillingim RB. Ethnic differences in thermal pain responses. Psychosom Med 1991;61:346–54.
[8] Evans KC, Banzett RB, Adams L, McKay L, Frackowiak RS, Corfield DR. BOLD fMRI identifies limbic, paralimbic, and cerebellar activation during air hunger. J Neuro-physiol 2002;88:1500–11.
[9] Gracely RH, Undem BJ, Banzett RB. Cough, pain and dyspnea: similarities and differences. Pulm Pharmacol 2007;20:433–7.
[10] Hagbarth KE, Kerr DI. Central influences on spinal afferent conduction. J Neurophysiol 1954;17:295–307.
[11] Harris G, Rollman GB. The validity of experimental pain measures. Pain 1983;17:369–76.
[12] Heath JR, Irwin CJ. An increase in breath-hold time appearing after breath-holding. Respir Physiol 1968;4:73–7.
[13] Lansing RW, Gracely RH, Banzett RB. The multiple dimensions of dyspnea: review and hypotheses. Respir Physiol Neurobiol 2009;167:53–60.
[14] McKay LC, Adams L, Frackowiak RS, Corfield DR. A bilateral corticobulbar network associated with breath holding in humans, determined by functional magnetic resonance imaging. Neuroimage 2008;40:1824–32.
[15] Millan MJ. Descending control of pain. Prog Neurobiol 2002;66:355–474.
[16] Morélot-Panzini C, Demoule A, Straus C, Zelter M, Derenne J-P, Willer J-C, Similowske T. Dyspnea as a noxious sensation: Inspiratory threshold loading may trigger diffuse noxious inhibitory controls in humans. Neurophysiology 2007;97:1396–404.
[17] Morin C, Bushnell MC. Temporal and qualitative properties of cold pain and heat pain: a psychophysical study. Pain 1998;74:67–73.
[18] Nishino T, Sugimori K, Ishikawa T. Changes in the period of no respiratory sensation and total breath-holding time in successive breath-holding trials. Clin Sci 1996;91:755–61.
[19] Nishino T, Isono S, Ishikawa T, Shinozuka N. Sex differences in the effect of dyspnea on thermal pain threshold in young healthy subjects. Anesthesiology 2008;109:1100–6.
[20] Pattinson KT, Governo RJ, MacIntosh BJ, Russell EC, Corfield DR, Tracey I, Wise RG. Opioids depress cortical centers responsible for the volitional control of respiration. J Neurosci 2009;29:8177–86.
[21] Peiffer D, Poline JB, Thivard L, Aubier M, Samson Y. Neural substrates for the perception of acutely induced dyspnea. Am J Respir Crit Care Med 2001;163:951–7.
[22] Rainville P, Duncan GH, Price DD, Carrier B, Bushnell MC. Pain affect encoded in human anterior cingulated but not somatosensory cortex. Science 1997;277:968–71.
[23] Price DD. Psychological and neural mechanisms of the affective dimension of pain. Science 2000;288:1769–72.
[24] Schön D, Dahme B, von Leupoldt A. Associations between the perception of dyspnea, pain, and negative affect. Psychophysiology 2008;45:1064–7.
[25] Shea SA, Andres LP, Shannon DC, Guz A, Banzett RB. Respiratory sensations in subjects who lack a ventilatory response to CO_2. Respir Physiol 1993;93:203–19.
[26] Sritippayawan S, Hamutcu R, Kun SS, Ner Z, Ponce M, Keens TG. Mother–daughter transmission of congenital central hypoventilation syndrome. Am J Respir Crit Care Med 2002;166:367–9.
[27] Strauser LM, Helikson MA, Tobias JD. Anesthetic care for the child with congenital central alveolar hypoventilation syndrome (Ondine's curse). J Clin Anesth 1999;11:431–7.
[28] Strigo IR, Duncan GH, Boivin M, Bushnell MC. Differentiation of visceral and cutaneous pain in the human brain. J Neurophysiol 2003;89:3294–303.
[29] Tracey I, Ploghaus A, Gati JS, Clare S, Smith S, Menon RS, Matthews PM. Imaging attentional modulation of pain in the periaqueductal gray in humans. J Neurosci 2002;22:2748–52.
[30] Tracey I. Imaging pain. Brit J Anaesth 2008;101:32–9.
[31] Treede RD, Kenshalo DR, Gracely RH, Jones AK. The cortical representation of pain. Pain 1999;79:105–11.
[32] von Leupoldt A, Sommer T, Kegat S, Baumann HJ, Klose H, Dahme B, Büchel C. The unpleasantness of perceived dyspnea is processed in the anterior insula and amygdala. Am J Respir Crit Care Med. 2008;177:1026–32.
[33] von Leupoldt A, Sommer T, Kegat S, Eipert F, Baumann HJ, Klose H, Kahme B, Büchel C. Down-regulation of insular cortex responses to dyspnea and pain in asthma. Am J Respir Crit Care Med 2009;180:232–8.